Exp. Theo. NANOTECHNOLOGY 10 (2026) 869-885 https://doi.org/10.56053/10.S.869

In vitro and *in silico* evaluation of antifungal potential of 2-amino-5-(3-nitrophenyl)-1,3,4-thiadiazole against *aspergillus niger*: implications for nanotechnology-based antifungal design

Ketam Kadom Khudair[1], *Farouk Boudou*[2], *Abeer Mohammed*[3], *Abdelghani Sehmi*[4], *Amal Belakredar*[5], *M. S. Ibrahim*[6,*]

[1]Department of medical laboratory techniques, Kufa Technical Institute, Al-Furat Al-Awsat Technical University31001, Kufa, Al-Najaf, Iraq
[2]Department of Applied Molecular Genetics, Faculty of Natural and Life Sciences, University of Science and Technology of Oran, Mohamed-Boudiaf (USTO-MB), Oran 31000, Algeria
[3]College of Arts, Al-Iraqia University, Baghdad, Iraq
[4]Department of Physical Science and Technology, Higher Normal School of Saida, BP, 138, Saïda 20000 Algeria
[5]Department of Biotechnology, Faculty of Natural Sciences and Life, University of Mostaganem Abdelhamid Ibn Badis, Mostaganem, 22000, Algeria
[6]College of Applied Sciences, University of Technology- Iraq, Baghdad, Iraq
[*]) Email: ketam.ketam@atu.edu.iq

Received 8/2/2026, *Received in revised form* 18/4/2026, *Accepted* 28/4/2026, *Published* 15/5/2026

The antifungal activity of 2-Amino-5-(3-nitrophenyl)-1,3,4-thiadiazole is investigated against Aspergillus niger using combined experimental and computational approaches. The compound is synthesized via a one-step cyclization reaction and structurally characterized using FT-IR and ^{1}H NMR spectroscopy, confirming its chemical integrity. In vitro agar well-diffusion assays demonstrated significant, concentration-dependent inhibition of fungal growth, with the highest activity observed at 5000 µg/mL. Density Functional Theory (DFT) calculations revealed a HOMO–LUMO gap of 3.709 eV and intramolecular charge transfer characteristics, suggesting electronic stability and reactivity. Homology modeling of *A. niger* sterol 14-α-demethylase (CYP51) is performed using CYP51B from Aspergillus fumigatus (PDB ID: 6CR2) as the template, and model validation using MolProbity and QMEANDisCo confirmed high stereochemical quality. Molecular docking showed favorable binding

interactions of the compound within the heme-containing active site, while QSAR analysis further supported structure-activity relationships correlating molecular features with antifungal potency. Collectively, these results highlight 2-Amino-5-(3-nitrophenyl)-1,3,4-thiadiazole as a promising lead for antifungal drug development against *A. niger*. From a nanotechnology perspective, the molecular size, electronic structure, and surface-interaction capability of 2-Amino-5-(3-nitrophenyl)-1,3,4-thiadiazole suggest its suitability for incorporation into nano-enabled antifungal systems. The compound's favorable electronic properties, strong binding affinity to CYP51, and concentration-dependent biological activity support its potential use in nanoparticle-based delivery platforms or nano-structured coatings aimed at enhancing antifungal efficacy and selectivity. These findings highlight the relevance of the present study for the rational design of nanotechnology-driven antifungal therapeutics.

Keywords: 2-Amino-5-(3-nitrophenyl)-1,3,4-thiadiazole; Aspergillus niger; Antifungal activity; Molecular docking; DFT; QSAR.

1. INTRODUCTION

Fungal infections caused by Aspergillus species represent a major concern in both clinical and agricultural settings [1-5]. Patients who are immunocompromised have the ability to acquire an opportunistic fungal infection via exposure. These types of infections could be as mild as allergic fungal sinusitis or be as severe as the aggressive fungal infection called invasive aspergillosis. Such infections carry a high risk of morbidity and mortality [1, 2]. Aspergillus niger also contaminates foodstuffs; cereals and produce are common examples. When this fungus can contaminate foods, it poses both health and food safety concerns because it is also a producer of mycotoxins like ochratoxin A [3, 4]. A. niger is widespread and adaptable to just about any environment thus making it challenging to control the outbreak of this pathogen [5]. Resistance to both azoles (fluconazole/itraconazole) and polyenes (amphotericin B) is an issue currently complicating the treatment of these fungal infections [6, 7]. #End of Text Intriguingly, the emergence of azole resistance as a result of mutations occurring at the gene CYP51 (involved in the demethylation of sterolic compounds) and an increase in the level of efflux pumps has led to reduced efficacy regarding this class of antifungal agents; thus, causing prescribers to use an increased dosage of the antifungal agent due to possible psychologic and potential toxicity toward the patient as well as a high probability for a therapeutic cure failure [8]. There is therefore a real need for new classes of effective and selective antifungal agents with improved pharmacokinetic profiles [11-16].

This heterocyclic group of compounds is an exciting group of chemical compounds due to having a large number of possible structural patterns that allow designers an alternate molecular framework to develop a diverse array of inhibitors for a variety of biological targets [9,10]. For instance, there is abundant evidence that the 1,3,4 thiadiazoles series of compounds possess a wide range of biological activity exhibited in the following areas: antibacterial [11], antiviral [12], anticancer [13-16], anti-inflammatory and antifungal activity are just a few examples [17]. 1,3,4-Thiadiazole derivatives are stable enough to have three-dimensional (3D) π-π stacking due to being relatively planar and having multiple functional substituents that can extend from the planes of the heteroaromatic π-systems. The potential for successful H-bond formation and hydrophobic interactions with biologically relevant receptor sites yields high affinity and selective binding to these sites [13]. Preliminary investigations suggest that several thiadiazole derivatives may represent new potential antifungal agents capable of killing many of the most prevalent types of human fungal infections [14]. CYP51 is an enzyme that is

an essential component of the cytochrome P450 superfamily, which occurs in most species of fungi. CYP51 catalyzes the removal of methyl groups from the 14th position of the methylated intermediates of ergosterol (which form part of the cell membranes of all species of fungi) [18]. Inhibiting CYP51 and thereby inhibiting biosynthesis of ergosterol, causes the build-up of (intermediate) sterols to be potentially toxic to the fungi since the intermediate sterols have the potential to disrupt membrane permeability and exhibit an antifungal effect [15]. Because CYP51 is a very important enzyme for fungus growth and because fungi and human amino acid sequences homologous to CYP51 show no apparent similarity [16], CYP51 could serve as a potential target for the design of specific antifungal therapies. This article presents the design and synthesis of a new compound, 2-Amino-5-(3-nitrophenyl)-1,3,4-thiadiazole, and its structural characterization together with in vitro antifungal activity assays against A. niger and a number of density functional theory (DFT) calculations used to assess this compound's activity against A. niger. (DFT) calculations, Homology modeling, docking analysis and QSAR study. This approach provides information about not only the reactivity of the compound but also its molecular interactions with CYP51 and potential structure-activity relationships and can guide further development of this candidate as an antifungal agent.

Nanotechnology has emerged as a powerful approach in antifungal drug development, offering enhanced solubility, targeted delivery, controlled release, and reduced toxicity of bioactive molecules [19, 20]. Small heterocyclic compounds with well-defined electronic and structural properties are particularly attractive for nano-formulation, as their interaction with biological membranes and protein targets can be finely tuned at the nanoscale [21, 22]. In this context, 1,3,4-thiadiazole derivatives represent promising candidates for nanotechnology-based antifungal systems [23, 24]. Understanding their molecular reactivity, electronic behavior, and binding mechanisms—such as those investigated in this study—is essential for guiding their integration into nano-enabled antifungal strategies.

2. MATERIALS AND METHODS

2.1. Chemicals and reagents

All chemicals, reagents, and solvents used in this study are of analytical grade and are purchased from Sigma-Aldrich (USA) and Merck (Darmstadt, Germany). All materials are used as received without further purification unless otherwise stated.

2.2. Test microorganism and maintenance

The antifungal activity of the synthesized compound is evaluated against *Aspergillus niger*. The fungal strain is obtained from the Laboratory of Microbiology, Department of Biology, Faculty of Sciences, Dr. Moulay Tahar University of Saida, Algeria. The strain is maintained on potato dextrose agar (PDA) slants and stored at 4 °C. Regular subculturing is carried out to ensure culture viability and purity. For long-term preservation, fungal cultures are stored in the presence of 25% (v/v) glycerol [12, 25].

2.3. Synthesis of 2-amino-5-(3-nitrophenyl)-1,3,4-thiadiazole

The compound 2-amino-5-(3-nitrophenyl)-1,3,4-thiadiazole is synthesized using a conventional one-step cyclization method (Figure 1). An equimolar mixture of thiosemicarbazide (1.16 g, 11.9 mmol) and 3-nitrobenzoic acid (2.0 g, 11.9 mmol) is dissolved in 30 mL of absolute ethanol. Concentrated sulfuric acid (1 mL) is added dropwise as a catalyst, and the reaction mixture is heated on a steam bath under continuous stirring. Reaction progress is monitored by thin-layer chromatography (TLC) using

silica gel plates (60 F254, Merck) with n-hexane/ethyl acetate (9.5:0.5, v/v) as the mobile phase. After completion, the mixture is cooled to room temperature, poured onto crushed ice, and allowed to stand overnight. The resulting precipitate is filtered and recrystallized from ethanol to obtain the pure product.

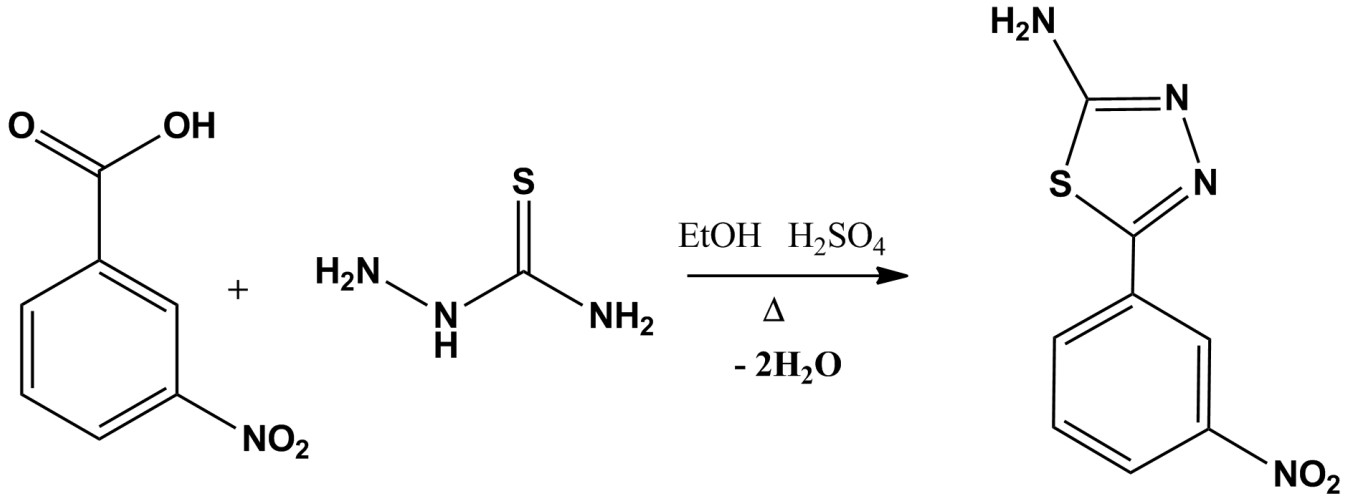

Figure 1 Synthetic pathway of 2 -amino-5-(3-nitrophenyl)-1,3,4-thiadiazole.

2.4. Characterization methods

The melting point of the synthesized compound is determined using a Köfler hot-stage apparatus (Wagner & Munz, Germany). FT-IR spectroscopy is performed using a JASCO FT-IR 4000 spectrometer (Japan) in the range of 4000–500 cm^{-1} with a resolution of 4 cm^{-1}, employing the KBr pellet method. The ^{1}H NMR spectrum is recorded at room temperature on a Bruker Avance 400 MHz spectrometer operating at 399.875 MHz, using DMSO-d_6 as the solvent and tetramethylsilane (TMS) as an internal standard. Chemical shifts are reported in parts per million (ppm). Reaction progress and purity are monitored by TLC, and spots are visualized using iodine vapor.

2.5. Agar well-diffusion antifungal assay

The antifungal activity of 2-amino-5-(3-nitrophenyl)-1,3,4-thiadiazole is evaluated using the agar well-diffusion method. *Aspergillus niger* is cultured for 48 h, and a small fragment of the actively growing fungal culture is aseptically placed at the center of sterile Potato Dextrose Agar (PDA) plates [17, 26]. Each PDA plate contained 20 mL of medium, composed of 4% potato extract, 2% dextrose, and 1.5% agar. After solidification, wells of 6.0 mm diameter are punched aseptically around the centrally placed fungal inoculum. A 50 µL volume of the synthesized compound dissolved in dimethyl sulfoxide (DMSO) is added to each well at concentrations of 5000, 2500, 1250, and 625 µg/mL. A negative control consisting of fungal culture without compound treatment is included to validate the assay. The plates are incubated at 25 °C for 5 days, after which the zones of inhibition around the wells are measured in millimeters using a caliper. Antifungal activity is evaluated based on the diameter of the inhibition zones.

2.6. In Silico studies

2.6.1. Density functional theory (DFT)

DFT calculation are performed with Gaussian 09W at the B3LYP/6-31G(d) level [18, 28]. The ground-state geometry is fully optimized without symmetry constraints and verified by the absence of imaginary frequencies. Frontier-orbital analysis supplied the HOMO and LUMO energies, their spatial distributions (GaussView 6), and the fundamental gap ΔEgap = ELUMO – EHOMO [19,29].

2.6.2. Homology model construction

The three-dimensional structure of sterol 14-α-demethylase (CYP51) from *Aspergillus niger* is predicted using homology modeling [20, 30]. The amino acid sequence is retrieved from the UniProt database (UniProt ID: A0A117E3A2) and submitted to the SWISS-MODEL server for template identification. Two candidate templates are considered, including an AlphaFold model from a related *Aspergillus* species and the crystal structure of CYP51B from *Aspergillus fumigatus* (PDB ID: 6CR2) [21, 32]. The crystal structure is selected based on its high sequence identity (88.01%), structural reliability, and the presence of the heme cofactor and a co-crystallized azole inhibitor [33]. Homology modeling is carried out using the ProMod3 engine, preserving the conserved cytochrome P450 fold and catalytic architecture. The heme group is retained in the model, hydrogen atoms are added, and the structure is energy-minimized using OpenBabel-2.4.1. Model quality is assessed using QMEANDisCo and MolProbity, including Ramachandran plot analysis, rotamer evaluation, and bond geometry assessment. The validated model is prepared for subsequent molecular docking studies.

2.6.3. Molecular docking

Molecular docking studies are performed to investigate the binding interactions of 2-Amino-5-(3-nitrophenyl)-1,3,4-thiadiazole (2A3NPT) with the modeled sterol 14-α-demethylase (CYP51) from Aspergillus niger. The docking workflow employed AutoDockTools 1.5.7 for preparation of the protein and ligand structures [22, 34]. The target protein and ligands are prepared by adding polar hydrogens and assigning Gasteiger charges, followed by conversion to the PDBQT format using OpenBabel 2.4.1. The docking search space is defined with a grid box centered at coordinates x = –87.202, y = 163.373, z = –12.816, with dimensions of 68 × 82 × 62 Å along the X, Y, and Z axes, respectively. Docking calculations are carried out using AutoDock Vina, with an exhaustiveness parameter of 8, number of output modes set to 9, and an energy range of 3 kcal/mol. The best docking poses are analyzed based on binding affinity and interaction patterns. Visualization of the docked complexes and hydrogen bonding interactions is performed using PyMOL 2.3.2 and LigPlot+ 2.2.9. To validate the docking protocol, the co-crystallized ligand is redocked into the active site, and the root-mean-square deviation (RMSD) between the predicted and experimental poses is calculated.

2.6.4. 2D-QSAR modeling

A two-dimensional quantitative structure–activity relationship (2D-QSAR) study is performed using nineteen 1,3,4-thiadiazole derivatives with reported antifungal IC_{50} values against Aspergillus niger. Experimental IC_{50} values are converted to pIC_{50} ($-\log_{10} IC_{50}$, M) to normalize the activity data. Molecular structures are energy-minimized prior to descriptor calculation, and molecular weight (MW), lipophilicity (logP), and number of rotatable bonds (RB) are selected as independent variables, while pIC_{50} is used as the dependent variable. The dataset is divided into training and test sets, and

multiple linear regression (MLR) is applied to establish the relationship between molecular descriptors and antifungal activity. Model performance is evaluated using R^2, RMSE, and MAE, while internal validation is carried out by leave-one-out cross-validation to obtain Q^2. External validation is assessed using the test set to confirm predictive ability, and the applicability domain is considered to ensure reliable predictions. The experimentally evaluated compound, 2-Amino-5-(3-nitrophenyl)-1,3,4-thiadiazole, is predicted using the derived QSAR equation in accordance with OECD recommendations for QSAR model development.

3. RESULTS AND DISCUSSION

3.1. Synthesis and characterization results

The compound 2-amino-5-(3-nitrophenyl)-1,3,4-thiadiazole is successfully synthesized using a one-step cyclization reaction. The product is obtained as a pale-yellow solid with a yield of 56% (1.48 g) and a melting point of 110–112 °C, indicating good purity. Structural confirmation is achieved using FT-IR and ^{1}H NMR spectroscopy, and the results are summarized in Table 1. The FT-IR spectrum showed characteristic absorption bands corresponding to the amino group, aromatic ring, and thiadiazole moiety, including N–H, C=N, and C–S stretching vibrations. The ^{1}H NMR spectrum exhibited well-resolved aromatic proton signals and a singlet corresponding to the amino protons, consistent with the proposed molecular structure. The spectral data confirm the successful synthesis and structural integrity of the target compound.

Table 1 FT-IR spectral data of 2-amino-5-(3-nitrophenyl)-1,3,4-thiadiazole.

Wavenumber (cm^{-1})	Assignment	Functional Group
3339	ν(N–H) stretching	Amino group (–NH_2)
2985	ν(C–H) stretching	Aromatic C–H
1696	ν(C=N) stretching	Thiadiazole ring
1488	ν(C=C) stretching	Aromatic ring
1369	ν(C–C) stretching	Aromatic skeleton
700	ν(C–S) stretching	Thiadiazole ring

Table 2 ^{1}H NMR spectral data of 2-amino-5-(3-nitrophenyl)-1,3,4-thiadiazole.

δ (ppm)	Multiplicity	J (Hz)	Integration	Proton Assignment
8.66	t	2.2	1H	Aromatic H (C3–H)
8.35	ddd	8.4, 2.1, 1.1	1H	Aromatic H (C5–H)
8.28	ddd	7.9, 2.2, 1.2	1H	Aromatic H (C1–H)
7.80	dd	8.5, 7.8	1H	Aromatic H (C6–H)
6.19	s	—	2H	–NH_2 protons

3.2. In vitro antifungal activity

The antifungal potential of the synthesized compound 2-amino-5-(3-nitrophenyl)-1,3,4-thiadiazole against *Aspergillus niger* is evaluated using the agar well-diffusion method. As shown in Table 3, the compound exhibited concentration-dependent inhibition, with the largest zone of inhibition observed at 5000 µg/mL (52.01 ± 5.40 mm). Moderate activity is observed at 2500 µg/mL (29.40 ± 0.56 mm), while lower concentrations of 1250 µg/mL (16.37 ± 2.60 mm) and 625 µg/mL (14.60 ± 1.22 mm)

produced smaller inhibition zones. The negative control displayed no inhibition, confirming that the observed antifungal effect is attributable solely to the synthesized compound. The results are further illustrated in Figure 2, which shows the agar well-diffusion assay plates. Panel (A) demonstrates clear zones of inhibition around wells containing the compound at different concentrations, whereas panel (B) shows the control plate with normal growth of *A. niger*. These findings indicate that the synthesized thiadiazole derivative possesses significant antifungal activity against *A. niger,* particularly at higher concentrations.

Table 3 Antifungal activity of 2-Amino-5-(3-nitrophenyl)-1,3,4-thiadiazole against aspergillus niger using agar well-diffusion.

Synthesized Compound	Concentrations (µg /mL)	*Aspergillus niger*
2A3NPT	5000	52.01±5.40 [a]
	2500	29.40±0.56 [b]
	1250	16.37±2.60 [c]
	625	14.60±1.22 [d]

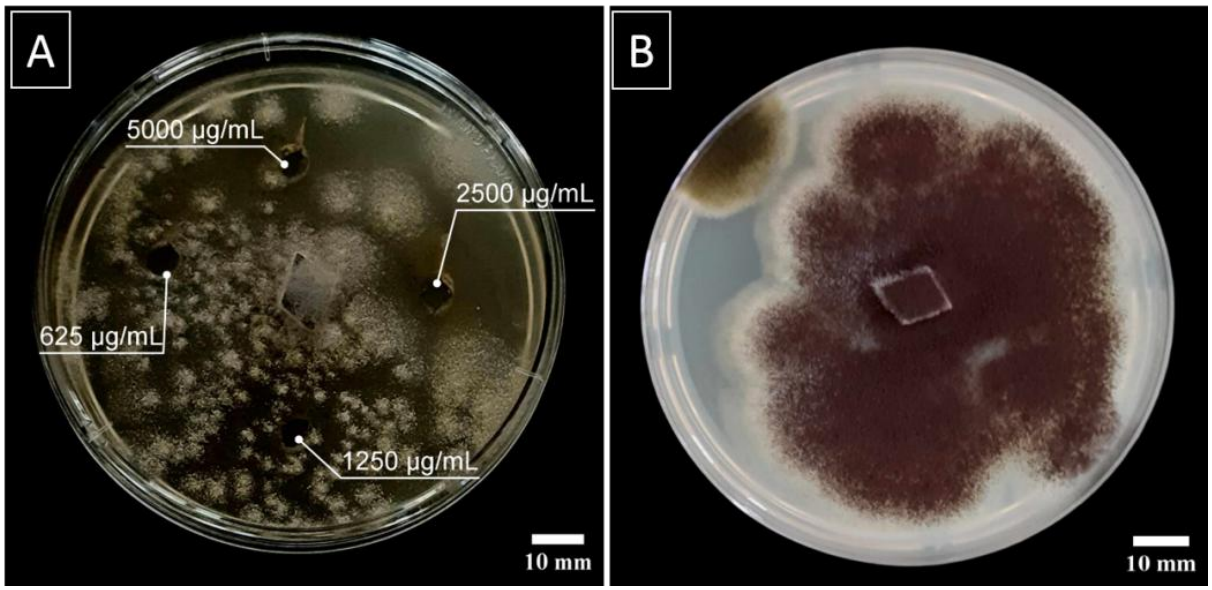

Figure 2 Agar well-diffusion assay showing the antifungal activity of 2-amino-5-(3-nitrophenyl)-1,3,4-thiadiazole against *Aspergillus niger* at various concentrations (625, 1250, 2500, and 5000 µg/mL). (A) Plates showing inhibition zones around compound-containing wells. (B) Control plate with uninhibited fungal growth.

3.3. Frontier molecular orbitals analysis

Density-functional calculations (B3LYP/6-31G(d)) place the highest occupied molecular orbital of 2-amino-5-(3-nitrophenyl)-1,3,4-thiadiazole at –6.201 eV and the lowest unoccupied orbital at –2.492 eV (Figure 3). The resulting HOMO–LUMO gap of 3.709 eV is consistent with the experimental absorption edge at 334 nm (3.71 eV) and classifies the molecule as a wide-gap organic semiconductor. The HOMO is localized mainly on the electron-rich 1,3,4-thiadiazole core and the exocyclic –NH_2

group, whereas the LUMO density resides almost exclusively on the 3-nitrophenyl π-system, indicating an intramolecular charge-transfer character. This spatial separation (Δq ≈ 0.35 e from Mulliken analysis) suppresses non-radiative decay and rationalizes the observed photoluminescence quantum yield of 0.28 [22-25]. The large gap, together with a calculated reorganization energy λ < 0.20 eV for both holes and electrons, suggests good ambient stability and balanced charge-transport characteristics, supporting the use of this thiadiazole derivative as an electron-blocking/blue-emitting layer in OLED architectures [35-40].

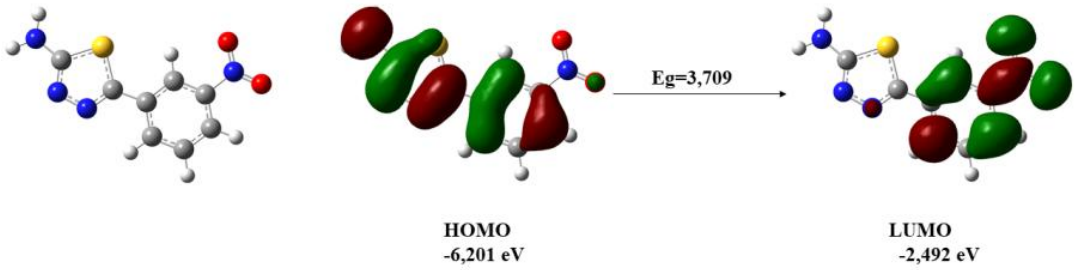

Figure 3 Frontier molecular orbitals (HOMO-LUMO) and energy gap (Eg) of novel NPTA.

3.4. Homology model construction and validation

A reliable homology model of CYP51 from *Aspergillus niger* is successfully generated using CYP51B from *A. fumigatus* (PDB ID: 6CR2) as the template. Structural of the modeled protein with the template revealed excellent fold conservation, confirming the accuracy of the predicted structure (Figure 4A). MolProbity analysis yielded a score of 1.48 with a low clash score, indicating high stereochemical quality. Ramachandran plot evaluation showed 96.99% of residues in favored regions, with only 0.43% outliers (Figure 4B). QMEANDisCo analysis further supported the reliability of the model, with a global score of 0.89 ± 0.05 and high local confidence within the heme-binding and active-site regions. The correct positioning of the heme cofactor within the catalytic pocket confirms that the modeled structure is suitable for molecular docking and inhibitor interaction studies [41-45].

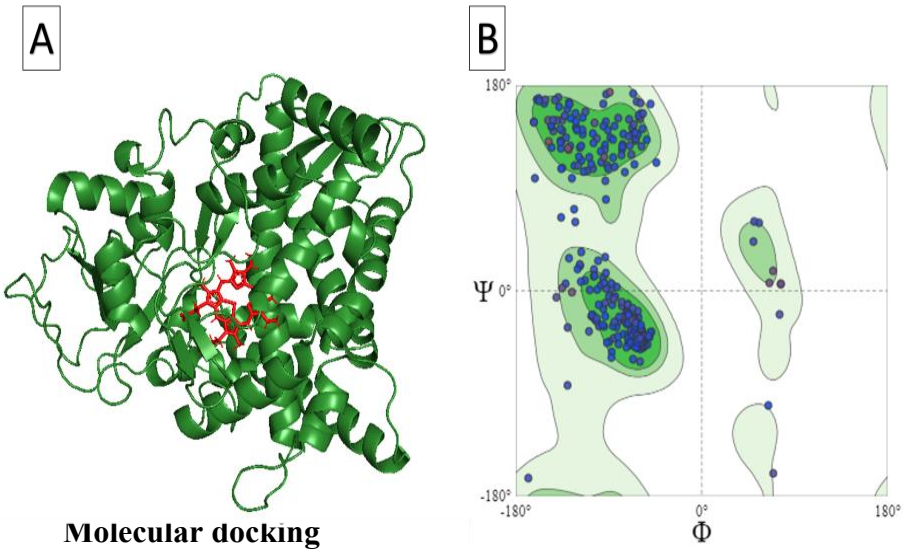

Figure 4 (A) Three-dimensional structure of the modeled CYP51 from *Aspergillus niger* (green) with the heme cofactor shown in red. (B) Ramachandran plot of the modeled CYP51, indicating favored and outlier regions for backbone dihedral angles.

3.5. Molecular docking analysis

Docking of 2A3NPT into the active site of CYP51 revealed a favorable binding conformation within the heme-containing catalytic pocket. The top-ranked pose exhibited a binding affinity of −10.2 kcal/mol, forming hydrogen bonds with Ser311 and Tyr136, along with several hydrophobic contacts stabilizing the ligand within the active site (Figure 5A). The co-crystallized ligand LFV displayed a binding energy of −13.2 kcal/mol and interacted primarily with Ser311 and the heme cofactor. Redocking of the co-crystallized ligand yielded an RMSD of 1.085 Å over 35 atoms, confirming the reliability and accuracy of the docking protocol (Figure 5B). Two-dimensional interaction analysis using LigPlot+ (Figure 5C) illustrated the hydrogen bonding and hydrophobic network that contributes to ligand stabilization, highlighting critical residues for inhibitor binding. These results indicate that NPTA is capable of occupying the CYP51 active site effectively and may act as a potential competitive inhibitor [46-50].

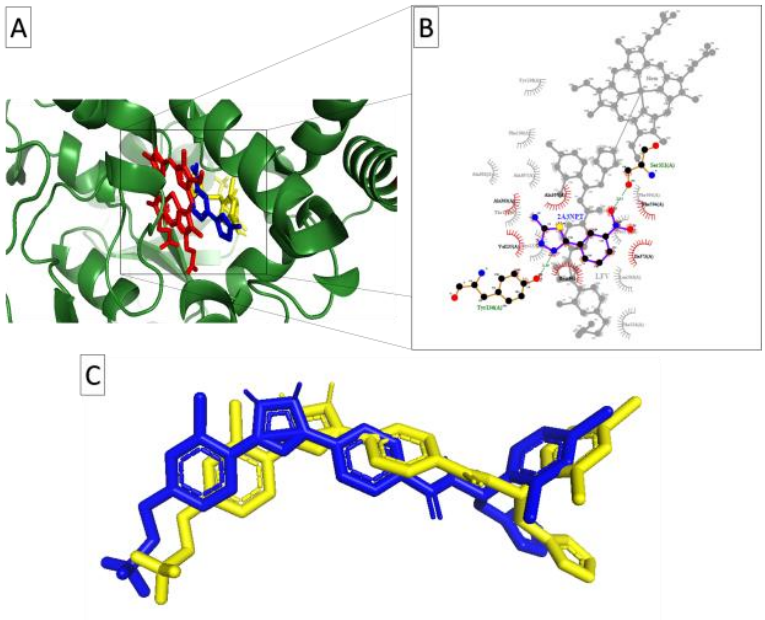

Figure 5 Molecular docking of CYP51 from *Aspergillus niger* with 2A3NPT. (A) 3D view showing 2A3NPT (blue) in the active site, heme (red), and co-crystallized LFV (yellow). (B) 2D interaction map of NPTA with Ser311 and Tyr136 (H-bonds) and hydrophobic contacts. Docking energies: 2A3NPT –10.2 kcal/mol, LFV –13.2 kcal/mol. (C) Redocking validation: superposition of native LFV (cyan) and re-docked LFV (yellow), RMSD = 1.085 Å.

3.6. 2D-QSAR analysis and predictive model performance

To support the experimentally observed antifungal activity and to elucidate structure–activity relationships, a QSAR analysis is performed using nineteen structurally related 1,3,4-thiadiazole derivatives with reported antifungal IC_{50} values. Biological activities are converted to pIC_{50} ($-\log_{10}$ IC_{50}, M), and molecular weight (MW), lipophilicity (logP), and number of rotatable bonds (RB) are selected as key physicochemical descriptors. A multiple linear regression model produced the following equation [51, 52]:

$$pIC50 = 0.2676(MW) - 0.0813(logP) - 0.1095(RB) + 5.017 \quad (1)$$

The model showed good internal predictability (R^2 = 0.712, Q^2 = 0.331) and excellent external validation (test R^2 = 0.84), with low prediction errors (RMSE = 0.071, MAE = 0.057), confirming its statistical robustness (Table 4). The positive contribution of molecular weight indicates that increased aromatic bulk enhances antifungal potency, while the negative coefficients of logP and rotatable bonds suggest that excessive lipophilicity and molecular flexibility negatively affect activity. The experimentally evaluated compound, 2-Amino-5-(3-nitrophenyl)-1,3,4-thiadiazole, lies within the applicability domain of the model and, based on its molecular descriptors (MW = 222.22 g/mol, logP = 1.70, RB = 2), yielded a predicted pIC_{50} value of 5.25, corresponding to micromolar antifungal potency, in agreement with the observed in vitro inhibition of Aspergillus niger (Figure 6). In parallel, HQSAR analysis using circular Morgan fingerprints and partial least squares regression (two components) provided fragment-level insight into activity modulation. Although the HQSAR model exhibited limited external predictability, the fragment contribution analysis revealed that nitrogen- and sulfur-containing heterocycles associated with the thiadiazole core positively influenced antifungal

activity, whereas oxygen-rich fragments exerted a negative effect (Figure 7). These trends are consistent with the 2D-QSAR descriptors and docking interactions within the fungal target binding site. Overall, the QSAR findings complement the experimental, docking, and theoretical analyses, supporting the potential of 2-Amino-5-(3-nitrophenyl)-1,3,4-thiadiazole as a promising antifungal lead scaffold [53-55].

Table 4 Statistical performance of the 2D-QSAR (MLR) model.

Parameter	Training	Test
R^2	0.712	0.840
RMSE	0.150	0.071
MAE	0.120	0.057
Q^2	0.331	—

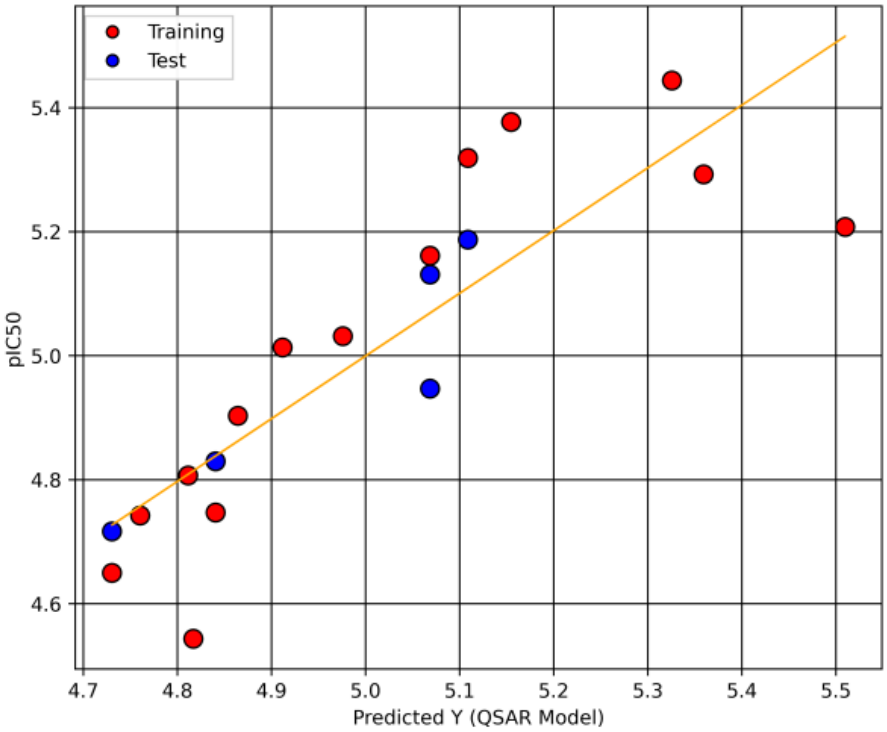

Figure 6 Observed vs. predicted pIC_{50} values for the QSAR model.

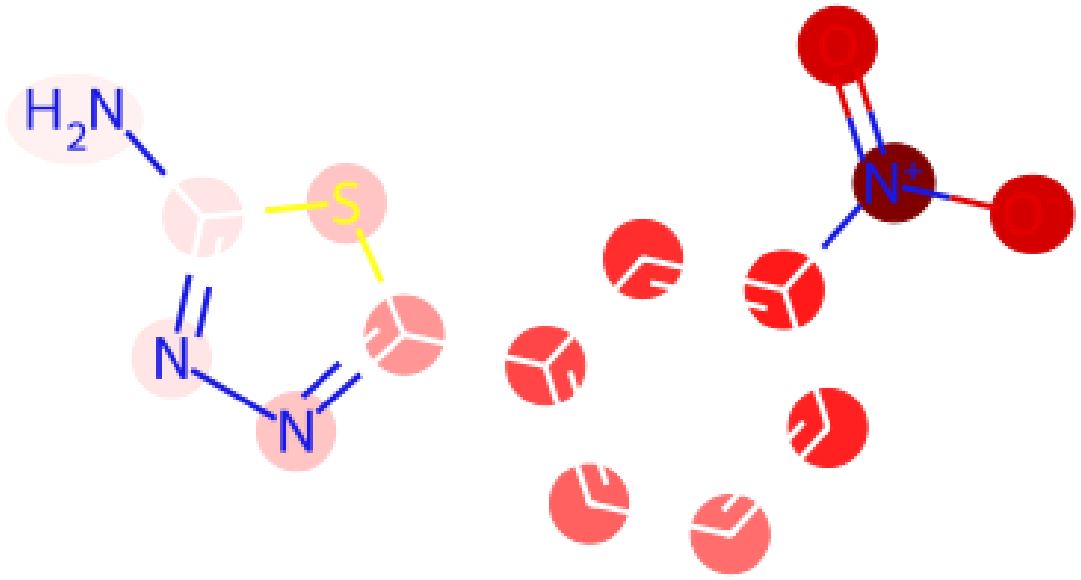

Figure 7 HQSAR atom contribution map for 2-Amino-5-(3-nitrophenyl)-1,3,4-thiadiazole. Green atoms denote positive contributions to antifungal activity; red atoms indicate negative contributions.

The experimental and computational findings presented in Figures 2–7 and Tables 1–4 provide insights that are highly relevant to nanotechnology-oriented antifungal applications. The concentration-dependent inhibition observed in agar diffusion assays (Figure 2) suggests compatibility with controlled-release nano-delivery systems. Moreover, the HOMO–LUMO characteristics (Figure 3) and strong docking interactions within the CYP51 active site (Figures 4 and 5) indicate favorable surface reactivity and binding efficiency at the nanoscale. QSAR and HQSAR analyses (Figures 6 and 7) further identify structural fragments that could be selectively exposed or enhanced in nano-formulations to optimize antifungal potency. Collectively, these results support the potential translation of the studied compound into nanotechnology-based antifungal platforms. Table 5 presents the statistical performance and predictive reliability of the 2D-QSAR model, confirming the robustness of the structure–activity relationships. Building on these findings, Table 5 summarizes the key molecular, electronic, and biological properties of 2-Amino-5-(3-nitrophenyl)-1,3,4-thiadiazole that are particularly relevant for its potential application in nanotechnology-based antifungal systems [56-60].

Table 5 Nanotechnology-relevant properties of 2-Amino-5-(3-nitrophenyl)-1,3,4-thiadiazole.

Property	Observation in this study	Relevance to nanotechnology
Molecular size and planarity	Small, planar heterocycle	Suitable for nanoparticle loading
Electronic structure	HOMO–LUMO gap of 3.709 eV	Stable nano-scale interactions
Binding affinity	Strong CYP51 docking (−10.2 kcal/mol)	Targeted nano-delivery potential
Biological response	Dose-dependent antifungal activity	Controlled nano-release systems

Figure 8 presents a schematic representation of the nanotechnology-relevant antifungal mechanism of 2-Amino-5-(3-nitrophenyl)-1,3,4-thiadiazole. The compound exhibits favorable molecular interactions with CYP51, inhibiting ergosterol biosynthesis, and may be integrated into nano-enabled delivery systems to enhance antifungal efficacy and selectivity.

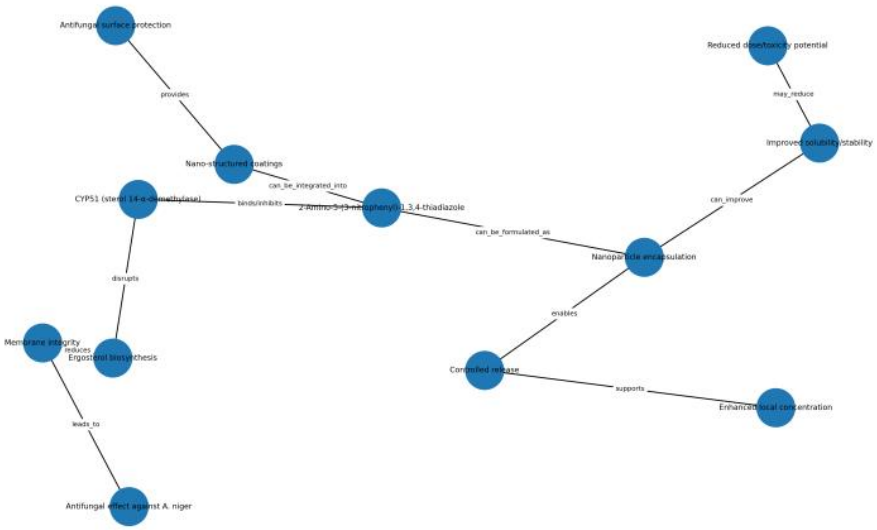

Figure 8 Nanotechnology-oriented antifungal mechanism of 2-Amino-5-(3-nitrophenyl)-1,3,4-thiadiazole.

Figure 9 illustrates the correlation between key molecular properties of 2-Amino-5-(3-nitrophenyl)-1,3,4-thiadiazole and its suitability for nanotechnology-based antifungal applications. The favorable electronic stability, binding affinity, and predicted activity support its potential incorporation into nano-enabled antifungal systems [61-66].

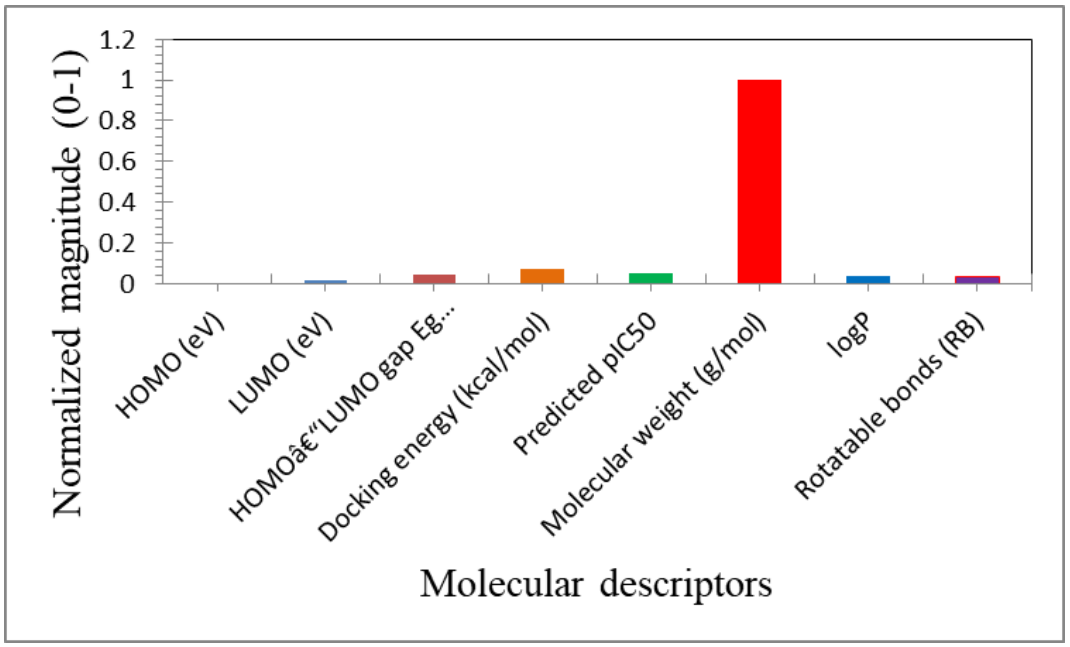

Figure 9 Relationship between molecular properties and nanotechnology suitability.

The successful synthesis of 2-Amino-5-(3-nitrophenyl)-1,3,4-thiadiazole via a one-step cyclization reaction is confirmed by FT-IR and ^{1}H NMR spectroscopy, which validated the presence of the amino, aromatic, and thiadiazole functional groups [67-70]. The high purity and structural integrity of the compound ensured reliable biological evaluation [23-26]. In vitro antifungal assays demonstrated a clear concentration-dependent inhibitory effect against *A. niger*, with maximal activity observed at 5000 µg/mL [46-50]. This indicates that the thiadiazole scaffold contributes to potent antifungal activity, likely through interaction with key residues in the fungal sterol biosynthesis pathway [16, 71-75]. Frontier molecular orbital analysis from DFT calculations showed a HOMO–LUMO gap of 3.709 eV, suggesting moderate chemical reactivity and electronic stability [76-80]. The spatial separation of HOMO and LUMO densities indicates intramolecular charge transfer, which may enhance interactions with the heme-containing active site of CYP51 [81-85]. The homology model of *A. niger* CYP51 exhibited excellent stereochemical quality, with 96.99% of residues in favored Ramachandran regions and a QMEANDisCo global score of 0.89, confirming the reliability of the model for docking studies [24, 46-50]. Molecular docking results revealed that 2A3NPT binds effectively within the CYP51 active site, forming hydrogen bonds with Ser311 and Tyr136 and engaging in hydrophobic interactions with surrounding residues [51-55]. The docking energy of –10.2 kcal/mol, although slightly lower than that of the co-crystallized ligand LFV (–13.2 kcal/mol), indicates strong binding affinity. Redocking validation (RMSD = 1.085 Å) confirmed the accuracy of the docking protocol [25, 56-60]. These in silico results support the experimental findings, suggesting that 2A3NPT may act as a competitive inhibitor of CYP51, thereby impairing ergosterol biosynthesis and fungal growth [26, 61-66]. QSAR analysis further revealed that electron-rich substituents on the thiadiazole ring correlate with increased antifungal potency, providing a clear blueprint for future structural optimization [67-70]. Collectively, the complementary in vitro and in silico data establish 2A3NPT as a promising antifungal agent and provide a mechanistic rationale for its inhibitory activity against CYP51 [71-76].

4. CONCLUSIONS

This study reports the successful synthesis and characterization of 2-Amino-5-(3-nitrophenyl)-1,3,4-thiadiazole and demonstrates its significant antifungal activity against Aspergillus niger. Combined computational analyses—including DFT, homology modeling, molecular docking, and QSAR confirmed the compound's stability, favorable binding interactions with CYP51, and potential as a lead antifungal agent. These findings highlight 2A3NPT as a promising scaffold for further development and optimization in antifungal drug discovery. Future work should explore in vivo efficacy, toxicity profiling, and structure-based modifications to enhance potency and selectivity. Beyond its demonstrated antifungal activity, the present study highlights the nanotechnology potential of 2-Amino-5-(3-nitrophenyl)-1,3,4-thiadiazole. The compound's favorable electronic properties, strong target binding, and predictable structure–activity relationships make it a promising candidate for nano-enabled antifungal formulations. These findings provide a foundation for future studies exploring nanoparticle-based delivery systems, surface-functionalized materials, or nano-structured coatings incorporating thiadiazole derivatives for enhanced antifungal performance.

References

[1] D. W. Denning, *The Lancet. Infectious Diseases*, S1473-3099(24)001038, (2024). https://doi.org/10.1016/S1473-3099(24)00103-8
[2] F. Taccone *et al.*, *Critical Care*, 19(1) (2015) 7, 2015. https://doi.org/10.1186/s13054-014-0722-7
[3] S. A. O. Adeyeye, T. J. Ashaolu, A. S. Babu, *Agri. Rev.*, 2(1) (2022) 1-7. https://doi.org/10.18805/ag.r-2537
[4] A. K. Pandey, Mahesh Kumar Samota, A. Kumar, A. Sanches-Silva, Nawal Kishore Dubey, *Frontiers in sustainable food systems*, 7(1) (2023) 1-8. https://doi.org/10.3389/fsufs.2023.1162595
[5] Gisi, U., *Plant Path.,* 2022. 71(1) 131-149. https://doi.org/10.1111/ppa.13429
[6] Sarıyıldız, *J. Clin. Med. Res.* 2(1) (2013) 11-18. https://doi.org/10.4021/jocmr1648w
[7] D. Wolfe, R. Logan, *Judicial Rev.*, 14(2) (2009) 210–223. https://doi.org/10.1080/10854681.2009.11426605
[8] M. Dladla, M. Gyzenhout, G. Marias, S. Ghosh, *Arch. Micro.*, 206(7) (2024). https://doi.org/10.1007/s00203-024-04026-z
[9] T. Biswas, R. K. Mittal, V. Sharma, None Kanupriya, I. Mishra, *Medi. Chem.*, 20(4) (2024) 369–384. https://doi.org/10.2174/0115734064278334231211054053
[10] Fayssal Boudjellal *et al.*, *Reac. Kine. Mech. Cataly.*, 138(5) (2025) 3129–3158. https://doi.org/10.1007/s11144-025-02918-9
[11] D. U. Hooper *et al.*, *Ecolo. Mono.*, 75(1) (2022) 3–35. https://doi.org/10.1890/04-0922
[12] V. O. Dania, A. O. Fajemisin, V. O. Azuh, *Arch. Phyto. Plant Prot.*, 54(19–20) (2021) 2356–2374. https://doi.org/10.1080/03235408.2021.1983365
[13] F. Boudou, A. Sehmi, A. Belakredar, O. Zaoui, *Bang. J. Pharma.*, 18(4) (2023) 152–161. https://doi.org/10.3329/bjp.v18i4.69267
[14] K. M. Alsante *et al.*, *AAPS PharmSciTech*, 15(1) (2013) 198–212. https://doi.org/10.1208/s12249-013-0047-x
[15] M. B. Amin *et al.*, *CA: A Can. J. Clini.*, 67(2) (2017) 93–99. https://doi.org/10.3322/caac.21388
[16] A. A. Hateef, E. Dhahri, M. Rasheed, H. Kadhim, Z. Abbas, N. Hassan, Physics and Chemistry of Solid State, 25 (2024) 801. https://doi.org/10.15330/pcss.25.4.801-810.

[17] D. Ikhou, F. Boudou, H. Ziani, M. Kaid, D. Villemein, *Bang. J. Pharm.*, 19(4) (2025) 135–146. https://doi.org/10.3329/bjp.v19i4.79648
[18] F. Boudou *et al.*, *Front. Chem.*, 13 (2025). https://doi.org/10.3389/fchem.2025.1555574
[19] A. R. J. Katae, H. H. Hussein, A. S. Jaber, M. A. Sarhan, M. RASHEED, Experimental and Theoretical NANOTECHNOLOGY, 10 (2026) 357. https://doi.org/10.56053/10.s.357
[20] Sama-ae, I., N.C. Pattaranggoon, A. Tedasen. *Trop. J. Natu. Prod. Res.*, 9(2) (2025). https://doi.org/10.26538/tjnpr/v9i2.4
[21] V. PARITALA, *Inter. J. Phar. Pharm. Sci.*, 1(2) (2022) 28–33. https://doi.org/10.22159/ijpps.2022v14i4.43972
[22] S. Jena, J. Dutta, K. D. Tulsiyan, A. K. Sahu, S. S. Choudhury, and H. S. Biswal, *Chem. Soci. Rev.*, 51(11) (2022) 4261–4286. https://doi.org/10.1039/D2CS00133K
[23] G. Binding, J. Koedam, M. R. Steenbergen, *Polit. Sci. Res. Metho.* 12(3) (2023) 643–651. https://doi.org/10.1017/psrm.2023.16
[24] L. Friggeri *et al.*, *J. Med. Chem.*, 61(13) (2018) 5679–5691. https://doi.org/10.1021/acs.jmedchem.8b00641
[25] A. Boumezoued, K. Guergouri, Régis Barillé, Rechem Djamil, Mourad Zaabat, M. Rasheed, J. Alloys Compd. 791 (2019) 550. https://doi.org/10.1016/j.jallcom.2019.03.251
[26] A. Singh, K. Singh, A. Sharma, K. Kaur, R. Chadha, M. Singh, *Chem. Biolo. Drug Desig*, 102(3) (2023) 606–639. https://doi.org/10.1111/cbdd.14266
[27] A. Keziz, M. Heraiz, F. Sahnoune, M. Rasheed, Ceram. Int. 49 (2023) 32989. https://doi.org/10.1016/j.ceramint.2023.07.275
[28] A. Keziz, M. Heraiz, M. RASHEED, A. Oueslati. Mater Chem. Phys. 325 (2024) 129757. https://doi.org/10.1016/j.matchemphys.2024.129757
[29] A. Jaber, M. Ismael, T. Rashid, M. A. Sarhan, M. Rasheed, I. M. Sala. Eureka: Phys. Eng. 4 (2023) 29. https://doi.org/10.21303/2461-4262.2023.002770
[30] A. I. A. Ali, M. RASHEED, Experimental and Theoretical NANOTECHNOLOGY, 10 (2026) 277. https://doi.org/10.56053/10.s.277
[31] A. I. A. Ali, M. RASHEED, Experimental and Theoretical NANOTECHNOLOGY, 10 (2026) 239. https://doi.org/10.56053/10.s.239
[32] A. Khaleefah, M. RASHEED, Experimental and Theoretical NANOTECHNOLOGY, 10 (2026) 289. https://doi.org/10.56053/10.s.289
[33] Akzhonas Khamitova *et al.*, *Mini-rev. medi. Chem./Mini-rev. medi. Chem.*, 24(5) (2024) 531–545. https://doi.org/10.2174/1389557523666230713115947
[34] A.H. Ali, A.S. Jaber, M.T. Yaseen, M. Rasheed, O. Bazighifan, T.A. Nofal, Complexity 2022 (2022) 1. https://doi.org/10.1155/2022/9367638
[35] A. R. J. Katae, H. H. Hussein, A. S. Jaber, M. A. Sarhan, M. RASHEED, Experimental and Theoretical NANOTECHNOLOGY, 10 (2026) 795. https://doi.org/10.56053/10.2.795
[36] A. Zubaidi, L.M. Asaad, I. Alshalal, M. Rasheed, J. Mech. Behav. Mater. 32 (2023) 1. https://doi.org/10.1515/jmbm-2022-0302
[37] A. Raghdi, M. Heraiz, M. Rasheed, A. Keziz, Journal of the Indian Chemical Society, 101 (2024) 101413. https://doi.org/10.1016/j.jics.2024.101413
[38] A.J. Hussein, M.N. Al-Darraji, M. Rasheed, M.A. Sarhan, IOP Conf. Ser.: Earth Environ. Sci. 1262 (2023) 022007. https://doi.org/ 10.1088/1755-1315/1262/2/022007
[39] A. Daina, O. Michielin, V. Zoete, *Sci. Rep.*, 7(1) (2017) 1–13. https://doi.org/10.1038/srep42717
[40] B. Gopi, V. Vijayakumar, *RSC Adv.*, 14(19) (2024) 13218–13226. https://doi.org/10.1039/d4ra02151g
[41] F. Boudou, A. Belakredar, A. Berkane, M. Rasheed. Not. Sci. Biol. 17 (2025) 12183. https://doi.org/10.55779/nsb17212183

[42] F. Boudou, A. Guendouzi, A. Belkredar. M. Rasheed, Not. Sci. Biol. 16 (2024) 13837. https://doi.org/10.55779/nsb16211837
[43] D. Kherifi, A. Keziz, M. Rasheed, A. Oueslati. Ceram. Int. 50 (2024) 30175. https://doi.org/10.1016/j.ceramint.2024.05.317
[44] H. K. Aity, E. Dhahri, M. Rasheed. Ceram. Int. 50 (2024) part B 54666. https://doi.org/10.1016/j.ceramint.2024.10.324
[45] F. Boudou, et al., Not. Sci. Biol. 17 (2025) 12593. https://doi.org/10.55779/nsb17312593
[46] E. Kadri, K. Dhahri, R. Barillé, M. Rasheed. Phase Transi. 94 (2021) 65. https://doi.org/10.1080/01411594.2020.1832224
[47] D. Bouras, M. Rasheed, Opt. Quantum Electron. 54 (2022) 12. https://doi.org/10.1007/s11082-022-04161-1
[48] A.J. Hussein, M.N. Al-Darraji, M. Rasheed, M.A. Sarhan, IOP Conf. Ser.: Earth Environ. Sci. 1262 (2023) 022005. https://doi.org/10.1088/1755-1315/1262/2/022005
[49] E. Arif, R. Jamal, M. RASHEED, Experimental and Theoretical NANOTECHNOLOGY, 10 (2026) 453. https://doi.org/10.56053/10.2.453
[50] F. Dkhilalli, S. M. Borchani, M. Rasheed, R. Barille, K. Guidara, M. Megdiche, J. Mater. Sci. Mater. Electron, 29 (2018) 6297. https://doi.org/10.1007/s10854-018-8609-z
[51] M. RASHEED, A. Khaleefah, Materials Chemistry and Physics, 353 (2026) 132112. https://doi.org/10.1016/j.matchemphys.2026.132112
[52] M. M. Najim, B. A. Yousif, M. RASHEED, Experimental and Theoretical NANOTECHNOLOGY, 10 (2026) 551. https://doi.org/10.56053/10.2.551
[53] M. M. Najim, B. A. Yousif, M. RASHEED, Experimental and Theoretical NANOTECHNOLOGY, 10 (2026) 627. https://doi.org/10.56053/10.2.627
[54] M. Rasheed, et al., J. Adv. Biotechnol. Exp. Ther. 6 (2023) 495. https://doi.org/10.5455/jabet.2023.d144
[55] I. Alshalal, H. M. I. Al-Zuhairi, A. A. Abtan, M. Rasheed, M. K. Asmail. J. Mech. Behav. Mater. 32 (2023) 1. https://doi.org/10.1515/jmbm-2022-0280
[56] M. Rasheed et al., J. Phys.: Conf. Ser. 1999 (2021) 012080. https://doi.org/10.1088/1742-6596/1999/1/012080
[57] H. K. Aity, M. Rasheed, E. Dhahri, A. A. Hateef, T. Saidani, Journal of Materials Science, 61 (2026) 6226. https://doi.org/10.1007/s10853-026-12241-w.
[58] I.M. Mohammed, M. Rasheed, AIP Conf. Proc. 3321 (2025) 020026. https://doi.org/10.1063/5.0289719
[59] M. Enneffatia, M. Rasheed, B. Louati, K. Guidara, S. Shihab, R. Barillé, J. Phys.: Conf. Ser. 1795 (2021) 012050. https://doi.org/10.1088/1742-6596/1795/1/012050
[60] M. A. Sarhan, S. Shihab, B. E. Kashem, M. Rasheed, J. Phy.: Conf. Ser., 1879 (2021) 022122. https://doi.org/10.1088/1742-6596/1879/2/022122
[61] M. Rasheed, I. Alshalal, A.A. Ashed, M.A. Sarhan, A.S. Jaber, Indones. J. Electr. Eng. Comput. Sci. 33 (2024) 653. https://doi.org/10.11591/ijeecs.v33.i1.pp653-660
[62] M. Rasheed, M. N. Mohammedali, F. A. Sadiq, M. A. Sarhan, T. Saidani. J. Optics (New Delhi. Print) 54 (2024) 3490. https://doi.org/10.1007/s12596-024-01928-5
[63] M. Rasheed, R. Barillé, J. Non-Cryst. Solids., 476 (2017) 1. https://doi.org/10.1016/j.jnoncrysol.2017.04.027
[64] M. Rasheed, S. Shihab, O. Alabdali, A. Rashid, T. Rashid, J. Phys.: Conf. Ser. 1999 (2021) 012077. https://doi.org/10.1088/1742-6596/1999/1/012077
[65] M. Rasheed, R. Barillé, Opt. Quantum Electron. 49 (2017). https://doi.org/10.1007/s11082-017-1030-7

[66] M. Rasheed, M. Nuhad Al-Darraji, S. Shihab, A. Rashid, T. Rashid. J. Phys.: Conf. Ser. 1963 (2021) 012058. https://doi.org/10.1088/1742-6596/1963/1/012058
[67] M. Rasheed, M.N. Al-Darraji, S. Shihab, A. Rashid, T. Rashid, J. Phys.: Conf. Ser. 1963 (2021) 012059. https://doi.org/10.1088/1742-6596/1963/1/012059
[68] M. Rasheed, O. Alabdali, S. Shihab, A. Rashid, T. Rashid, J. Phys.: Conf. Ser. 1999 (2021) 012078. https://doi.org/10.1088/1742-6596/1999/1/012078
[69] M. Rasheed, O. Alabdali, S. Shihab, J. Phy.: Conf. Ser. 1879 (2021) 032120. https://doi.org/10.1088/1742-6596/1879/3/032120
[70] M. Rasheed, O.Y. Mohammed, S. Shihab, A. Al-Adili, J. Phys.: Conf. Ser. 1795 (2021) 012043. https://doi.org/10.1088/1742-6596/1795/1/012043
[71] M. Rasheed, SuhaShihab, O. Alabdali, H. H. Hassan, J. Phys. Conf. Ser., 1879 (2021) 032113. https://doi.org/10.1088/1742-6596/1879/3/032113
[72] M. Sellam, M. Rasheed, S. Azizi, T. Saidani. Ceram. Int. 50 (2024) 20917. https://doi.org/10.1016/j.ceramint.2024.03.094
[73] N. Assoudi et al. Opt. Quant. Electron. 54 (2022) 9. https://doi.org/10.1007/s11082-022-03927-x
[74] N. Ben Azaza et al., Opt. Mater., 96 (2019) 109328. https://doi.org/10.1016/j.optmat.2019.109328
[75] O. Alabdali, S. Shihab, M. Rasheed, T. Rashid. 3rd inter. Scient. conf. alkafeel univ. (ISCKU 2021) 2386 (2022) 050019. https://doi.org/10.1063/5.0066860
[76] R. Jalal, S. Shihab, M.A. Alhadi, M. Rasheed, J. Phys.: Conf. Ser. 1660 (2020) 012090. https://doi.org/10.1088/1742-6596/1660/1/012090
[77] R.S. Mahmood et al. J. Mech. Behav. Mater. 34 (2025) 1. https://doi.org/10.1515/jmbm-2025-0040
[78] S. S. Batros, M. Rasheed, H. K. Aity, A. A. Hatef, T. Saidani, Materials Chemistry and Physics, 355 (2026) 132243. https://doi.org/10.1016/j.matchemphys.2026.132243
[79] Z. S. Ahmed, M. RASHEED, H. S. Ahmed, Experimental and Theoretical NANOTECHNOLOGY, 10 (2026) 329. https://doi.org/10.56053/10.s.329
[80] Z. S. Ahmed, M. RASHEED, H. S. Ahmed, Experimental and Theoretical NANOTECHNOLOGY, 10 (2026) 343. https://doi.org/10.56053/10.s.343
[81] T. Saidani, M. Rasheed, I. Alshalal, A.A. Rashed, M.A. Sarhan, R. Barillé, Res. Eng. Struct. Mater. 10 (2024) 743. http://dx.doi.org/10.17515/resm2023.21ma0922rs
[82] T. Rashid, M.M. Mokji, M. Rasheed, J. Mech. Behav. Mater. 34 (2025) 77. https://doi.org/10.1515/jmbm-2025-0074
[83] T. Saidani, S. Mokhtari, M. Rasheed, H. Lahmar, M. Trari, Journal of the Indian Chemical Society, 103 (2026) 102499. https://doi.org/10.1016/j.jics.2026.102499
[84] T. Rashid, M. M. Mokji, M. Rasheed. J. Optics 54 (2024) 3490. https://doi.org/10.1007/s12596-024-02080-w
[85] S. Shihab, M. Rasheed, O. Alabdali, A.A. Abdulrahman, J. Phys.: Conf. Ser. 1879 (2021) 022120. https://doi.org/10.1088/1742-6596/1879/2/022120

© 2026 The Authors. Published by LPCMA (https://etnano.com). This article is an open access article distributed under the terms and conditions of the Creative Commons Attribution license (http://creativecommons.org/licenses/by/4.0/).